Training Toddlers Seated on Mobile Robots to Drive Indoors Amidst Obstacles

Xi Chen, Christina Ragonesi, Sunil K. Agrawal, James C. Galloway

Abstract—

The goal of this research is to train children seated on mobile robots to purposefully and safely drive indoors. Our previous studies show that in about six weeks of training, infants can learn to drive directly to a goal using conventional joysticks. However, they are unable to acquire the advanced skill to avoid obstacles while driving. This limits mobility impaired children from exploring their home environment safely, which in turn impacts their cognitive and social developments in the important early years.

In this paper, we describe results where toddlers are trained to drive a robot within an obstacle course. Using algorithms based on artificial potential fields to avoid obstacles, we create force field on the joystick that trains them to navigate while avoiding obstacles. In this 'assist-as-needed' approach, if the child steers the mobile robot outside a force tunnel centered around the desired direction, the driver experiences a bias force on the hand. The results suggest that force-feedback joystick results in faster learning than with a conventional joystick.

Index Terms—**Haptic Device, Force-feedback Joystick, Force Tunnels, Obstacle Avoidance, Driver Training.**

I. Introduction

OUR research is ultimately aimed at mobility training of infants, especially those that are developmentally delayed. In typically developing infants, the onset of crawling and walking has long been associated with changes across developmental domains such as cognition and perception ([10], [11]). Currently, infants born with significant mobility impairments do not use power mobility devices until they are three years of age [13] and this impacts their development. Our goal is to characterize the impact of early mobility training on perceptual, cognitive, and social skills of children [12], with our in-house designed intelligent mobility devices. The impact of early mobility training is just emerging. Our initial results indicate that perceptual, cognitive, and social skills in certain populations of special needs infants benefit through mobility training [14][15].

Although young infants were readily able to learn to drive our robots, early mobility training with a conventional joystick has indicated that infants are unable to develop higher-level driving skills, i.e., turning left/right, avoiding obstacles. This motivates our current research to study the effects of force feedback joystick on mobility training.

Today, haptic rendering has become a powerful tool to augment virtual reality [1]. Force-feedback joysticks are used in haptics to provide virtual reality [2], attain better device control ([3], [4], [5]), and provide human assistance ([4], [6], [7], [8], [9]). Different force effects have been used in haptics for feeling textures [5], simulating physical events [4], and perceiving obstacles [3]. A single wall effect is used to prevent a driver from running into an obstacle, and in the event of collision, vibration is triggered to simulate this event ([4],[6]). Sometimes, a constant force, independent of joystick lever position, is given to push a driver away from obstacles ([7], [8], [3]). A force from the nearest obstacle is used or a vector sum of repulsive forces from all obstacles is calculated. These strategies successfully provide assistance during movement. However, none of these studies have focused on skill learning in toddlers as a result of these strategies.

Several recent studies are concerning about skill learning under haptic guidance. In [21], researchers used a similar pre-test–training–post-test paradigm as our experiment for movement learning using a PHANToM device. In [22], a one-dimensional force with fading strength was implemented on a steering wheel to train adults to learn a steering task. The same strategy was also applied to children with average age 6.6 years old [23]. Independently, our previous study [24] also demonstrated the effectiveness of haptic guidance for directional driving on adults and children with special needs. It is important to point out salient differences with our work. (i) Subjects have both control on the forward and turning velocity. If we prescribe the robot translational velocity as [23], our child subjects are frightened without knowing why the robot is moving. (ii) The force field in our work is a two-dimensional field implemented on a force-feedback joystick, and only acts outside a cone centered around a nominal direction of a joystick motion, predicted by an error correcting control law. (iii) The subjects in our study are toddlers under three years old, some of whom are special needs children.

Fig. 1. A typical toddler classroom at the ELC with desks, chairs, and cabinets.

In this study, we train toddlers 26-34 months old to navigate and avoid obstacles, with or without force-feedback, in an environment (Fig. 3) mimicking the real world. Fig. 1

shows a toddler classroom in the Early Learning Center (ELC), at the University of Delaware. Children play in this area and interact with others.

Using a force-feedback joystick, if a human driver moves the mobile robot outside a force tunnel centered around the desired direction computed by an algorithm, the driver must overcome bias forces on the hand in order to continue to move away from the targeted direction. This force feedback from the joystick helps in error correction and training of drivers. The experiment results show that, although a few toddlers may be able to learn this behavior with conventional joysticks, the learning is expedited by the use of force field controllers.

The paper is organized as follows: Section II describes the experiment setup. Details of an autonomous obstacle avoidance and navigation algorithm is given in Section III. Force tunnels on the joystick are described in Section IV. Section V describes the group study on ten typically developing toddlers. Training results for a mobility impaired toddler with spina-bifida are presented in Section VI.

II. Experiment Setup

Fig. 2 shows the various modules of our experiment setup. The force-feedback joystick is an Immersion Impulse Stick, which can provide 8.5N continuous force and 14.5N peak force. The joystick control is through DirectX, which can read joystick input and set forces. The mobile robot is a two-wheel Pioneer3-DX robot equipped with encoders. All programs are written in C++ to interface with an onboard library which has access to current robot pose and obstacle free area.

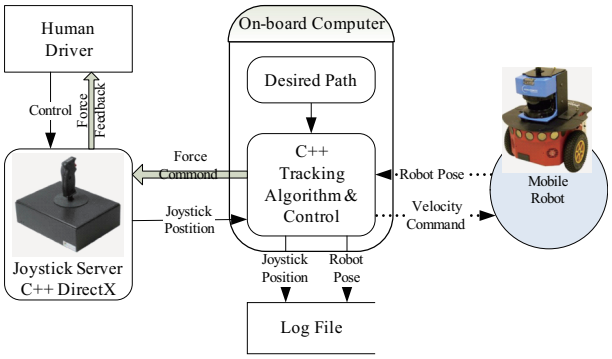

Fig. 2. A schematic of the experimental system setup

The training environment is constructed as shown in Fig. 3. Five walls represented by connecting the points $(0,0)-(0,6)$, $(2.8,0)-(2.8,6)$, $(0,1.5)-(1.4,1.5)$, $(1.4,3)-(2.8,3)$, $(0,4.5)-(1.4,4.5)$ are set up in this area. The child starts at point $(0.7,0)$. A experimenter stands at the goal $(0.7,6)$ with a toy to attract the child. The child achieves this goal by navigation while avoiding obstacles.

A robot could be made to autonomously navigate through this maze using a number of available control laws. However, the goal of this research is to train toddlers to drive the robot inside this maze, i.e., learn this navigation algorithm, using a force-feedback joystick. We use a potential field based controller[16] to implement the path planning and obstacle avoidance. The algorithm allows quick calculation of the desired driving direction from any point within the maze to the goal. Our hypothesis is that the human driver will be able to learn this control law, i.e., this navigation and obstacle avoidance strategy, over multiple training sessions via haptic feedback.

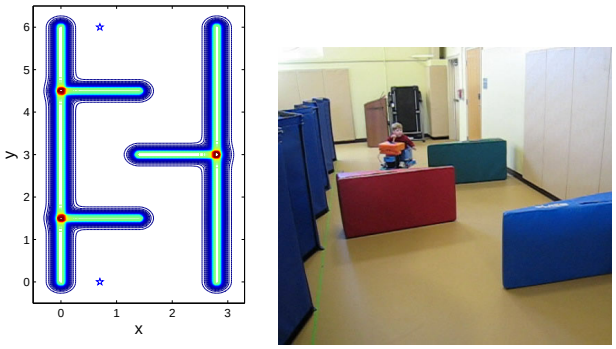

Fig. 3. Training Environment. ☆marks the start point and the goal point. This figure also shows the repulsive potential field.

III. Controller based on Potential Field

Using no-slip kinematics of the wheels, the states of the robot satisfy the following governing differential equations:

$$\begin{pmatrix} \dot{x}_c \\ \dot{y}_c \\ \dot{\theta} \end{pmatrix} = \underbrace{\begin{pmatrix} \cos\theta & 0 \\ \sin\theta & 0 \\ 0 & 1 \end{pmatrix}}_{Bu} \begin{pmatrix} v \\ \omega \end{pmatrix} \tag{1}$$

We choose an attractive potential field $U_a(x_c, y_c)$ due to the goal and a repulsive potential field $U_r(x_c, y_c)$ due to the obstacles, both independent of the robot orientation θ. Then the total potential function:

$$U(x_c, y_c) = U_a + U_r$$

is also independent of θ. This potential function is selected from the perspective of achieving only the goal position and not the orientation of the vehicle at the goal. We choose U such that it has only one global minimum at goal $\mathbf{p}_g = [x_g, y_g]$. With these chosen properties, $\frac{\partial U}{\partial \mathbf{p}_c} = 0$ if and only if

$$d = \|\mathbf{p}_c - \mathbf{p}_g\|_2 = \sqrt{(x_c - x_g)^2 + (y_c - y_g)^2} = 0$$

where $\mathbf{p}_c = [x_c, y_c]$.

In an earlier work, the gradient of such a potential function was used to control the rotational velocity of the vehicle [17]. A second study used this function in the development of a non-smooth controller [18]. Inspired by these, we propose the following control law:

$$u = -(K_1 B^T + K_2 F)\nabla U \tag{2}$$

where $K_1 = \begin{pmatrix} k_1 & 0 \\ 0 & k_1 \end{pmatrix}$, $K_2 = \begin{pmatrix} k_2 & 0 \\ 0 & k_2 \end{pmatrix}$, $k_1,\ k_2 > 0$, $\nabla U = \begin{pmatrix} \frac{\partial U}{\partial x_c} & \frac{\partial U}{\partial y_c} & 0 \end{pmatrix}^T$, $F = \begin{pmatrix} 0 & 0 & 0 \\ -\sin\theta & \cos\theta & 0 \end{pmatrix}$.

Now, consider the Lyapunov function $V = U$,

$$\begin{aligned} \dot{V} &= \nabla U^T B u = -\nabla U^T B(K_1 B + K_2 F)\nabla U \\ &= -k_1\left(\frac{\partial U}{\partial x_c}\cos\theta + \frac{\partial U}{\partial y_c}\sin\theta\right)^2 \\ &\leq 0 \end{aligned}$$

The invariant set [19] is defined by:

$$\begin{cases} \frac{\partial U}{\partial x_c}\cos\theta + \frac{\partial U}{\partial y_c}\sin\theta = 0 \\ (K_1 B^T + K_2 F)\nabla U = 0 \end{cases} \tag{3}$$

which gives:

$$\frac{\partial U}{\partial x_c} = 0,\ \frac{\partial U}{\partial y_c} = 0$$

With our assumption, there is only one global minimum. Hence, it must be at the goal, i.e., $d = 0$.

A. Selection of Potential Field

We choose the attractive potential field due to the goal as in [16]:

$$\begin{aligned} U_a(\mathbf{p}_c) &= \tfrac{1}{2}k_a \left\|\mathbf{p}_c - \mathbf{p}_g\right\|_2^2 \\ &= \tfrac{1}{2}k_a\left[(x_c - x_g)^2 + (y_c - y_g)^2\right] \end{aligned}$$

which is independent of the robot orientation θ. Its gradient is:

$$\nabla U_a(\mathbf{p}_c) = \begin{pmatrix} k_a(x_c - x_g) \\ k_a(y_c - y_g) \\ 0 \end{pmatrix}$$

For any obstacle $\mathcal{O}$, and for points $\mathbf{p}_o$ on the obstacle, define the measure of the distance from the robot to the obstacle $\mathcal{O}$ as:

$$\rho(\mathbf{p}_c) = \min_{\mathbf{p}_o \in \mathcal{O}} \left\|\mathbf{p}_c - \mathbf{p}_o\right\|_2^2$$

Define ρ_0, a positive constant, as the *radius of influence* from the obstacle. The repulsive potential field is selected as

$$U_r(\mathbf{p}_c) = \begin{cases} \frac{1}{2}k_r\left(\frac{1}{\rho(\mathbf{p}_c)} - \frac{1}{\rho_0}\right)^2 & \text{if} \rho(\mathbf{p}_c) \leq \rho_0 \\ 0 & \text{if} \rho(\mathbf{p}_c) > \rho_0 \end{cases}$$

which is also independent of θ. The gradient due to this obstacle is:

$$\nabla U_r(\mathbf{p}_c) = \begin{cases} -k_r\left(\frac{1}{\rho(\mathbf{p}_c)} - \frac{1}{\rho_0}\right)\frac{1}{\rho^2(\mathbf{p}_c)}\nabla\rho(\mathbf{p}_c) & \text{if} \rho(\mathbf{p}_c) \leq \rho_0 \\ 0 & \text{if} \rho(\mathbf{p}_c) > \rho_0 \end{cases}$$

B. Minima of the Potential Field

This choice of the potential field gives several local minima, as shown by equipotential curves in Fig. 4.

According to the earlier assumption, the potential field should have a single minimum in the region of interest. In order to achieve this, we divide the training area into four regions and place three intermediate goal points at $(2.1, 1.5)$, $(0.7, 3)$, and $(2.1, 4.5)$. Inside each region, the robot will pursue its designated goal point. Once the robot reaches close to an intermediate goal ($d < d_0$), the current goal is switched to the next. This process is repeated until the robot reaches the final goal point. Using this potential field based controller, the simulation results are shown in Fig. 5, where a robot successfully reaches a goal position starting out from an initial configuration.

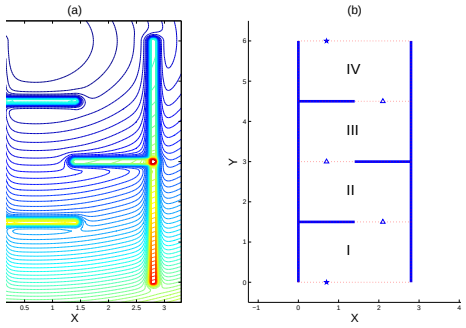

Fig. 4. (a) Equipotential curves within the training area, with at least two local minima around points $(0.7, 1.2)$ and $(0.7, 4.2)$. (b) Division of the training area into four regions. Three intermediate goals are added at the point $(2.1, 1.5)$, $(0.7, 3)$, and $(2.1, 4.5)$, marked by $\triangle$.

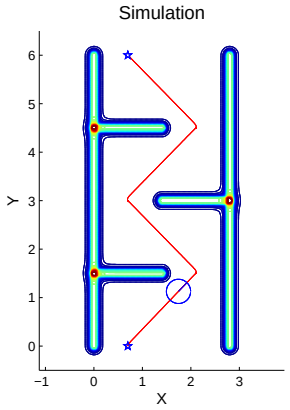

Fig. 5. Simulation result from initial state $(x_c, y_c, \theta) = (0.7, 0, \pi/2)$, with $d_0 = 0.26$ which is the robot swing radius. This figure shows only the potential field due to the obstacles.

IV. Creation of Force Tunnels

The control commands for v and ω, computed by Eq.(2), can be viewed as ideal commands which an autonomous driving algorithm would have imparted to the robot. However, in the experiments, the movement commands are given by the human driver through the joystick. Thus, given the mapping of velocity commands to the physical motion of the joystick, we set the instantaneous force tunnel for the joystick using these ideal v and ω commands.

A. Mapping of the Joystick Motion

The joystick in the experiment has predominantly two motions - forward/backward and left/right. In our exper-

iment, we associate pure forward/backward motion of the joystick to translational motion of the vehicle along the heading direction. The pure side to side motion of the joystick is associated with rotation of the vehicle. We scale the forward/backword joystick position using $v_{\max} = 0.36$ m/s and side to side joystick position using $\omega_{\max} = 26°/s$. Hence, given the desired control input v and ω from the controller Eq.(2), the ideal joystick movement direction, as shown in Fig. 6, is given by

$$\beta = \arctan(\frac{v}{v_{\max}} / \frac{\omega}{\omega_{\max}})$$

B. Force Tunnels around Nominal Joystick Motion

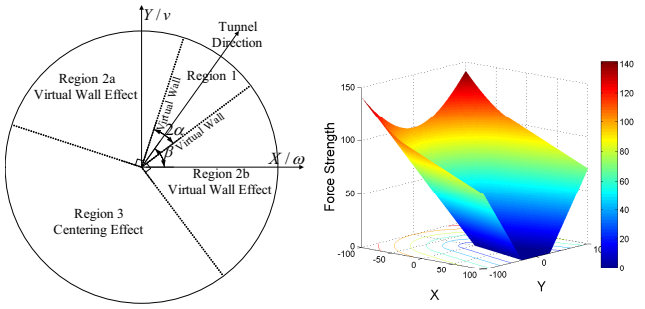

Fig. 6. (i) Force Tunnel shown by a virtual walls around Nominal Joystick Motion Direction, (ii) Tip force within the cone is zero. Tip force outside the cone for the tunnel direction $\beta = 0$ and half tunnel width $\alpha = 15°$. The damping effect not shown in these plots.

A cone angle of 2α is defined around the tunnel direction of joystick motion β computed in Section A. In the 'assist-as-needed' paradigm for training, no force field is applied on the hand, if the driver initiates a joystick motion within the cone. Fig. 6 (i) shows graphically four regions around this instantaneous direction of motion.

We define three force effects which qualitatively are:

1. *Virtual wall effect* - applies a restoring force to bring the handle of the joystick back to Region 1. This force is normal to the virtual wall and proportional to the distance from the wall. The unit vector along the virtual wall between Region 1 and Region 2a/2b is

$$\mathbf{w} = [\cos(\beta \pm \alpha),\ \sin(\beta \pm \alpha)]^T \tag{4}$$

Then the virtual wall effect can be represented by

$$\mathbf{F}_w = k_c[(\mathbf{p}_l^T \mathbf{w})\mathbf{w} - \mathbf{p}_l] \tag{5}$$

where $\mathbf{p}_l = [x_l, y_l]^T$ is the joystick handle position.

2. *Centering effect* - applies a restoring force to bring the joystick handle back to the center, represented by

$$\mathbf{F}_c = -k_c \mathbf{p}_l \tag{6}$$

k_c is selected so that when $\mathbf{p}_l$ reaches its max value, $k_c \mathbf{p}_l$ will be the max allowable force input in DirectX.

3. *Damping effect* - applies force on the joystick handle in a direction opposite to its displacement. This force prevents chattering of the joystick. Mathematically,

$$\mathbf{F}_d = -k_d[\dot{x}_l, \dot{y}_l]^T \tag{7}$$

where $\dot{x}_l, \dot{y}_l$ are the joystick tip speeds in the joystick frame. The coefficient k_d is selected to be the minimal value so that the joystick handle does not vibrate.

The haptic forces in the four regions of Fig. 6(i) are:

- Region 1: Damping effect only to stabilize the joystick, $\mathbf{F} = \mathbf{F}_d$.
- Region 2a & 2b: Vector sum of virtual wall and damping effects, $\mathbf{F} = \mathbf{F}_w + \mathbf{F}_d$.
- Region 3: Vector sum of centering and damping effects, $\mathbf{F} = \mathbf{F}_c + \mathbf{F}_d$.

A haptic force field with the above choice, is shown in Fig. 6 (ii). The z-coordinate represents the force magnitude. The x-y plane represents the joystick workspace. Please note that this choice of force field varies continuously over the joystick workspace and thus avoids any sharp and jerky changes in the force.

V. Driving Experiments and Results for Typically Developing Toddlers

Experiments were conducted with ten typically developing toddlers, randomly assigned into two groups. The training group included five toddlers with an average age 30.6 months, and were trained with the force field. The control group also included five toddlers with an average age 29.6 months, and were trained with no force field. The parents of all children signed the consent form approved by the University of Delaware Institutional Review Board.

The training protocol is as follows. The training consists of three stages. An experimenter stands at the goal $(0.7, 6)$ and uses toys to encourage the child to navigate to the goal.

- Stage 1 (Pre-training): Two trials without force field are collected on the first day for both groups. This serves as baseline data.
- Stage 2 (Training): This stage is divided into three non-consecutive days since the attention span of children is small. During each day, a toddler in the training group is trained with the force field for three trials. A fourth trial is collected without the force field. The control group complete four trials without the force field.
- Stage 3 (Final-test): In order to show that the toddlers have actually learned the driving behavior and not the specific course, we ask the children to drive from end to start in the absence of the force field. This requires a different sequence of moves. This is done one week after Stage 2 is complete.

If the child does not reach the goal in three minutes, this trial is considered as 'Failed', after which a new trial is started.

Robot position and travel time are recorded and used for comparisons. The number of obstacle collisions is also recorded during each trial. We propose two measurements to access the performance:

1. To compare the performance before, during, and after training, and between groups, we calculate the deviation area from the desired path from simulation (Fig. 5) by numerical integration shown in Fig. 7(a). This area is used as a measure for the performance

of both groups, since this desired path is a natural path that connects the goals in the training algorithm. Note this measurement will give penalty to redundant paths, which is a sign of inexpertness in driving, as shown by Fig. 7(b).

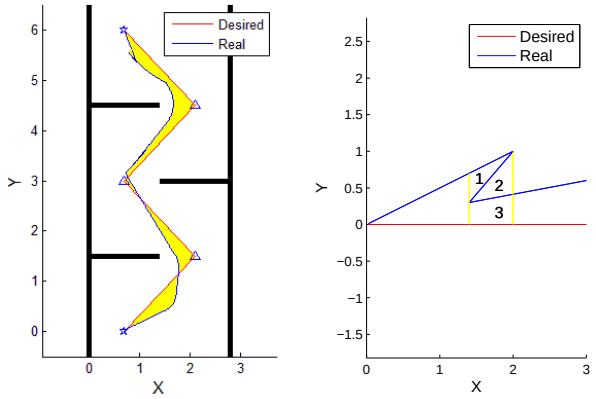

(a) Deviation Area (b) Redundant Path

Fig. 7. (a) An illustration of the deviation from the desired path with area 1.26m^2, shown in yellow. (b) Area 1, 2, and 3 are calculated once, twice and three times respectively due to the back and forth driving.

2. To measure if there is any changes of the correcting force provided during the training, we calculate total force for each trial from start ($t=0$) to finish ($t=t_f$) as:

$$W = \int_0^{t_f} F(t)dt \tag{8}$$

where $F(t)$ comes from the force field Eq.(5) and Eq.(6) at any instantaneous time. This measurement captures both the correcting force provided by the joystick and the time taken to finish each trial.

Fig. 8 shows the deviation area of the two groups. Fig. 9 shows the travel time data. Fig. 10 shows the total force calculated by Eq.(8) for the training group. Before any statistical analysis, all sets of data are tested for normality by Lilliefors test [20].

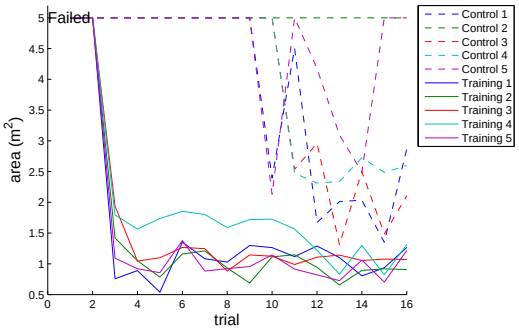

Fig. 8. Deviation Area of the two groups. Note trials 1-2 are the baseline. Trials 3-14 are the training trials. Trials 15-16 are the final test.

The following observations can be made from the data:

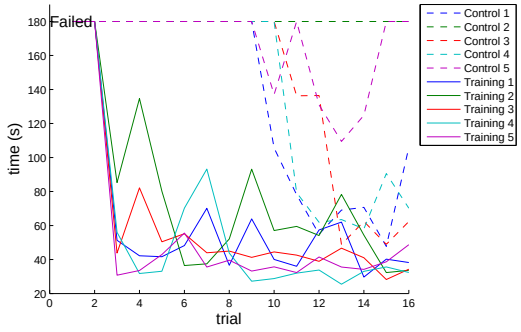

Fig. 9. Travel Time of the two groups

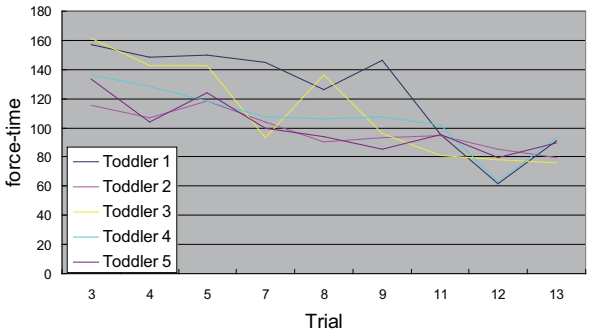

Fig. 10. Total force of the training group

1. During the baseline, none of the subjects could finish the task of navigating to the goal. They all failed during these first two trials (Fig. 11).

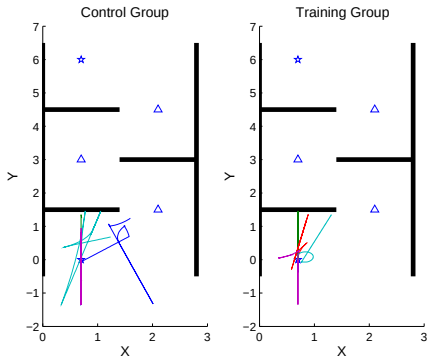

Fig. 11. First Trial of Baseline (Trial 1) of 10 Toddlers.

2. The force field significantly expedited the learning for the training group (t-test on the number of trials needed to succeed, $p=0.001$). When the force field was turned on, all subjects in the training group succeeded in reaching the goal. They maintained this behavior during all following trials. Only after nine or ten trials could a toddler in the control group succeed. It should be noted that the force field never actively push the joystick to the desired direction. Children need to find their way to the goal on their own.
3. The force field helps the toddler learn to navigate faster and more accurately. The deviation area of the

training group is significantly smaller than the control group after the training (Fig. 12, t-test on the last trial of the Stage 2, $p = 0.001$). The travel time is also significantly faster than the control group ($p = 0.03$).

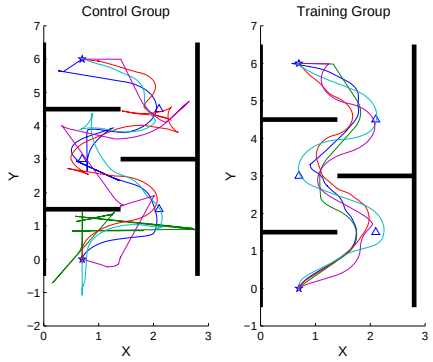

Fig. 12. Last Trial of Stage 2 (Trial 14) of 10 Toddlers.

4. For the training group, when the force field was on, the results were usually better, though not significantly. However if we compare the last trial of Day 1, Day 2, and Day 3, there was a significant decrease between each two days (paired t-test, $p = 0.001$ and 0.001 respectively). These results indicate that toddlers progressively learned to navigate and maintained this behavior even when the force field was off.
5. Total correcting force applied on the training group decrease significantly over the training trials (Fig. 10). Using linear regression, we find the coefficients are all negative (Table I).

TABLE I
LINEAR REGRESSION RESULTS

Toddler	Coefficient	R^2	p
1	-10.51	0.7336	0.0032
2	-4.41	0.8236	0.0007
3	-10.87	0.8019	0.0011
4	-6.74	0.7474	0.0026
5	-5.32	0.6741	0.0067

6. The force field also helps toddlers drive safely by assisting obstacle avoidance. Table II shows the average number of collisions in Trials 3-16 of the two groups ($p = 0.001$).

TABLE II
AVERAGE NUMBER OF COLLISIONS

Toddler	Training	Control
1	0	2.64
2	0	3.79
3	0	1.14
4	0	1.79
5	0	2.29

7. Once the toddlers made one successful trial to the goal, they maintained this behavior, even in the reversed course, except for one toddler in the control group who failed once after he made first successful trial and in the reversed course. All other children who succeeded to reach the goal with conventional joystick also succeeded in the final test (Fig. 13). However, both the deviation area and time of the training group were significantly smaller than the control group ($p = 0.005$ and 0.005 respectively).

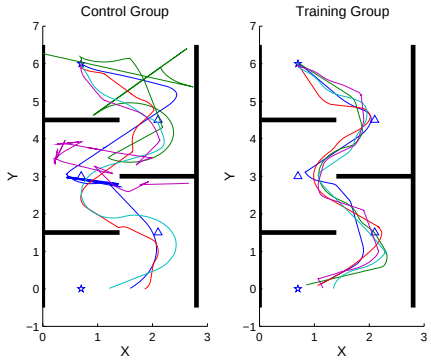

Fig. 13. Last Trial of Final Test (Trial 16) of 10 Toddlers.

VI. DRIVING EXPERIMENTS AND RESULTS OF A TODDLER WITH SPECIAL NEEDS

A 2-year old child with spina bifida received force field training. This child has good control of his hand movement, but lacks the ability to walk. The objective of this experiment is to test whether this force field can help the special needs child to learn navigation and drive more accurately. The learning is tested by pre and post training evaluation experiments in the absence of force field.

This child has been driving a standard power wheelchair since age one [14]. It is interesting to note that he also was able to benefit from the force-feedback joystick.

The training protocol is as follows: each day's training consists of four sessions. Each session has two trials. Total training lasts for 4 non-consecutive days. All other conditions are the same as the previous group study.

- Session 1 (Pre-training): This serves to collect the baseline of the subject. No force feedback is given.
- Session 2 & 3 (Training 1 & 2): The force field is turned on.
- Session 4 (Post-training): No force feedback is given.

As the group study, two trials without force field guidance were collected for the final test (denoted by Day 5) two weeks after Day 4 by reversing the course. This will show that the child has actually learned this driving behavior.

The same measure of deviation area is used, as well as the average time for each session. This time, if the child does not reach the goal in ten minutes, this trial is considered as 'Failed' and a new trial is begun.

Fig. 14 shows the deviation area between the reference and the actual paths. Fig. 15 shows the travel time data. Fig. 16 shows the total force over four days for the special needs child.

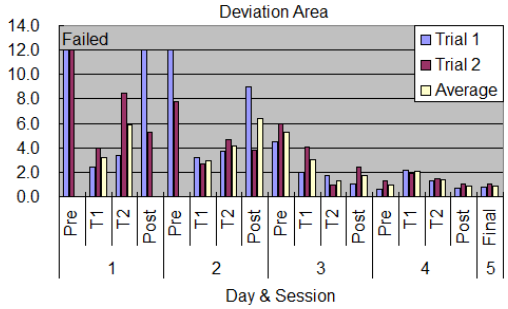

Fig. 14. Error from the reference path over five days of training and final test for the special needs child

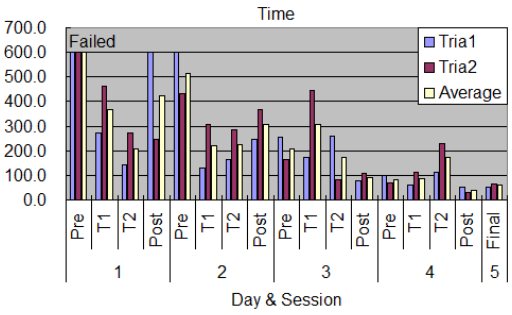

Fig. 15. Travel time over five days of training and final test for the special needs child

The following observations can be made from these data:

1. The training course was difficult enough that this child failed the first two trials. Yet he was able to learn to navigate and avoid obstacles finally.
2. The deviation area from the reference path significantly decreased in four days of training (Fig. 14). At the beginning of the training, the toddler could not navigate to the goal. On Day 4, the performance during both pre and post-training had improved drastically (Fig. 17).
3. When the force field was on, the child drove much better than the pre and post-training trials of the same day. While the child's performance improved, this trend became less significant.
4. One observes that for this case, the travel time decreased substantially over four days.
5. Total force applied decreased significantly over four day's training. Linear regression result shows the coefficient is significantly negative (Fig. 16).
6. In the final test, the child successfully navigated to the goal with similar performance as Day 4.

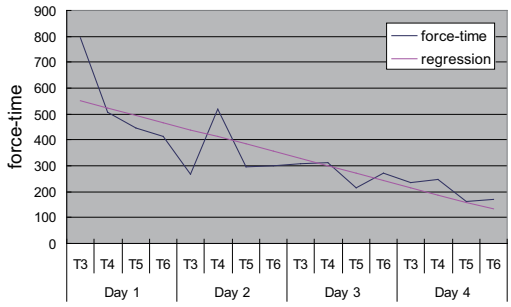

Fig. 16. Total force with linear regression results for the special needs child. Coefficient$= -27.94$, $R^2 = 0.6777$, $p = 0.0001$.

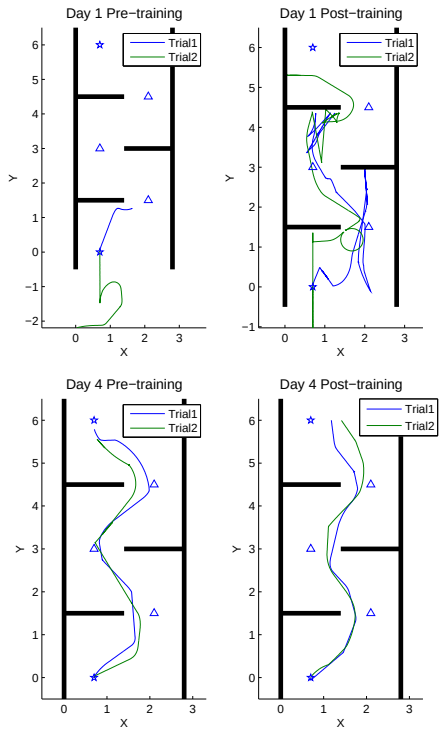

Fig. 17. Pre- and Post-training results of Day 1 and 4 for the special needs child

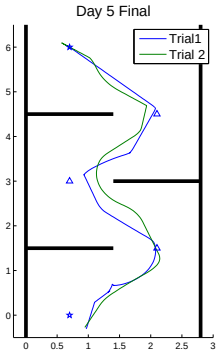

Fig. 18. Final Test for the special needs child

VII. Conclusion

In this paper, we present a novel force field to train toddler drivers to avoid obstacles while driving a mobile robot. These skills are necessary to navigate in more typical environments of home and classroom. A control law motivated from autonomous control of mobile robots was used and the toddlers were trained to learn this behavior using a force feedback joystick. Experiments were conducted in (i) a pilot group study and (ii) training of a special needs child driver with the force field. The results of the group study show that the force field algorithm helps very young

children learn to navigate and avoid obstacles faster, more accurately, and with greater safety. The results from the child with spina bifida support the use of a force-feedback joystick during practice with a child with mobility impairments.

On natural question to ask is if the toddlers just learnt the specifics of that path or they learned the behavior of avoiding obstacles and navigating to the goal via force field. Also, would the toddlers be able to retain this acquired skill later after the training is complete? In order to answer these questions, subjects were retested one week after the training was complete, but in a different configuration of maze. The results suggest that the toddlers were able to learn the behaviors and retain them at least one week after the training.

In the future, we will extend this novel application of technology and training to allow young children with special needs to explore using power mobility devices in real world environments such as their homes and classrooms.

References

[1] Lin, M., Salisbury, K., *Haptic rendering - beyond visual computing*, IEEE Computer Graphics and Applications, 24(2):22-23, 2004.

[2] Liao, Y., Chou, L., Horng, T., Luo, Y., Young, K., Su, S., *Force Reflection and Manipulation for a VR-based Telerobotic System*, Proc. Natl. Sci. Counc. ROC(A), Vol. 24, No. 5, 382-389, 2000.

[3] Han, S., Lee, J., *Tele-operation of a Mobile Robot Using a Force Reflection Joystick with a Single Hall Sensor*, 16th IEEE Inter. Conf. on Robot & Human Interactive Communication, Aug. 2007.

[4] Wang, X., Seet, G., Lau, M., Low, E., Tan, K.C., *Exploiting Force Feedback in Pilot Training and Control of an Underwater Robotics Vehicle: an Implementation in LabVIEW*, OCEANS 2000 MTS/IEEE Conference and Exhibition, Vol. 3, 2037-2042, 2000.

[5] Rujbio-Sierra, F.J., Stark, R.W., Thalhammer, S., Heckl, W.M., *Force-feedback Joystick as a Low-cost Haptic Interface for an Atomic-force-microscopy nanomanipulator*, Appl. Phys. A 76, 903-906, 2003.

[6] Luo, R.C., Hu, C., Chen, T., Lin, M., *Force Reflective Feedback Control for Intelligent Wheelchairs*, Proc. of the 1999 IEEE/RSJ Intl. Conf. on Intelligent Robots and Systems, 1999.

[7] Lee, S., Sukhatme, G.S., Kim, G.J., Park, C.M., *Haptic Control of a Mobile Robot: A User Study*, Proc. of the IEEE/RSJ Intl. Conf. on Intelligent Robots and Systems, Oct. 2002.

[8] Fattouh, A., Sahnoun, M., Bourhis, G., *Force Feedback Joystick Control of a Powered Wheelchair: Preliminary Study*, IEEE International Conference on Systems, Man and Cybernetics, 2004.

[9] Bourhis, G., Sahnoun, M., *Assisted Control Mode for a Smart Wheelchair*, Proc. of the IEEE 10th Intl. Conf. on Rehabilitation Robotics, June 12-15, 2007.

[10] Campos, J.J., Anderson, D.I., Barbu-Roth, M.A., Hubbard, E.M., Hertenstein, M.J., Witherington, D., *Travel Broadens the Mind*, Infancy, 1(2):149-219, 2000.

[11] Anderson, D.I., Campos, J.J., Anderson, D.E., Thomas, T.D., Witherington, D.C., Uchiyama, I., Barbru-Roth, M.A., *The flip side of perception-action coupling: locomotor experience and the ontogeny of visual-postural coupling*, Human Movement Science, Vol. 20, No. 4-5, 461-487, 2001.

[12] Galloway, J.C., Ryu, J.C., Agrawal, S.K., *Babies driving robots: self-generated mobility in very young infants*, Intel Serv Robotics 1(2):123C134, 2008.

[13] Teft, D., Guerette, P., Furumasu, J., *Cognitive predictors of young children's readiness for powered mobility*, Dev Med Child Neurol. 41(10):665-70, 1999.

[14] Lynch, A., Ryu, J.C., Agrawal, S.K., Galloway, J.C., *Power Mobility Training for a 7-month-old Infant with Spina Bifida*, Pediatric Physical Therapy, 21(4):362-368, 2009.

[15] Ragonesi, C., Chen, X., Agrawal, S.K., Galloway, J.C., *Power Mobility and Socialization in Preschool: A Case Report on a Child with Cerebral Palsy*, Pediatric Physical Therapy, 22(3):322-329, 2010.

[16] Latombe, J-C., *Robot Motion Planning*, Kluwer Academic Publishers, 1991.

[17] Borenstein, J., Koren, Y., *Real-time obstacle avoidance for fact mobile robots*, IEEE Transactions on Systems, Man and Cybernetics, Vol. 19, 1179-1187, 1989.

[18] Urakubo, T., Okuma, K., Tada, Y., *Feedback Control of a Two Wheeled Mobile Robot with Obstacle Avoidance Using Potential Functions*, Proceedlngs of IEEE International Conference on Intelligent Robots and Systems, Sep. 28 - Oct. 24, 2004.

[19] Slotine, J-J., Li, W., *Applied Nonlinear Control*, Prentice Hall, 1991.

[20] Lilliefors, H., *On the Kolmogorov-Smirnov test for normality with mean and variance unknown*, Journal of the American Statistical Association, Vol. 62. pp. 399-402, 1967.

[21] Bluteau, J., Coquillart, S., Payan, Y., Gentaz, E., *Haptic Guidance Improves the Visuo-manual Tracking of Trajectories*, PLoS ONE 3:e1775, 2008.

[22] Marchal-Crespo, L., Reinkensmeyer, D., *Haptic Guidance Can Enhance Motor Learning of a Steering Task*, Journal of Motor Behavior, 40(6):545-556, 2008.

[23] Marchal-Crespo, L., Furumasu, J., Reinkensmeyer, D.J., *A robotic wheelchair trainer: design overview and a feasibility study*, Journal of NeuroEngineering and Rehabilitation, 7:40, 2010.

[24] Agrawal, S.K. Chen, X., Galloway, J.C., *Training Special Needs Infants to Drive Mobile Robots Using Force-feedback Joystick*, In Proc. IEEE Int. Robotics and Automation Conf., May., 2010.